

IMAGING SYSTEMS WITH ALVAREZ-LOHMANN LENSES

Adrian Grewe and Stefan Sinzinger

Fachgebiet Technische Optik, IMN MacroNano®, Technische Universität Ilmenau

ABSTRACT

Luiz Alvarez and Adolf Lohmann independently invented specific kinds of varifocal lenses in the late 1960s. The focal length of these lenses is changed by a lateral displacement of two freeform phase plates. This enables compact optical systems with tunable focal length by using well defined surface functions. Due to the rapid development of precision fabrication technologies for freeform optical components in the last 20 years, Alvarez-Lohmann lenses became a current topic of research [1-4]. Typically the theory behind these lenses is based on an idealized model to describe the optical system. Since not all assumptions of the model are fulfilled in real optical systems, Alvarez-Lohmann lenses induce aberrations that decrease imaging quality. We analyze aberrations typical for Alvarez-Lohmann systems and suggest optical designs to increase the imaging quality of those systems. As an example for optimized Alvarez Lohmann systems a hyperspectral imaging system is presented.

Index Terms – Alvarez lenses; Lohmann lenses, tunable optics, hyper spectral

1. INTRODUCTION

Alvarez Lohmann lenses are freeform optical elements which realize a tunable optical function [5, 6]. In contrast to classical lens systems, the tuning effect is achieved by a relative lateral displacement of the elements. The well-defined description of the element function enables a high repeatability of the tuning. This makes the elements interesting for the design of compact varifocal optics. Furthermore the recent development of modern fabrication technologies, like diamond turning and milling or lithography, makes the fabrication of complex freeform elements possible [7, 8]. In the classical approach Alvarez Lohmann lenses are designed with a theoretical model, which assumes simplifications of the optical system. Fabricable systems do not fulfill these assumptions; hence aberrations are introduced into the optical system. In this paper these aberrations are analyzed and a method to compensate for them is proposed. Therefore the principle of Alvarez-Lohmann lenses is explained in section 2. The description used by Alvarez differs from the one proposed by Lohmann. In section 3 it is demonstrated, that both descriptions can be converted into each other. The aberrations which are introduced by a violation of the theoretical assumptions are presented in section 4. A model to analyze and compensate for these aberrations is proposed in section 5. In section 6 a hyperspectral imaging system using optimized Alvarez lenses is presented.

2. ALVAREZ-LOHMANN LENSES - THE PRINCIPLE OF OVERLAYING OPTICAL ELEMENTS

The principle of Alvarez Lohmann lenses is based on a differentiation similar to the difference quotient of a function. The first Alvarez Lohmann element features the negative function of the second ($f_1(x, y) = -f_2(x, y)$). Both elements are arranged in a manner that their

functions compensate for each other. If element 1 is shifted by $+\Delta$ and element 2 by $-\Delta$ the functions will not compensate each other. The resulting function is [9, 10]:

$$\Delta z(x, y) = f(x + \Delta x, y) - f(x - \Delta x, y) \quad (2.1)$$

$$\frac{\Delta z}{\Delta x} = \frac{f(x + \Delta x, y) - f(x - \Delta x, y)}{2\Delta x} \quad (2.2)$$

Compared with the symmetric difference quotient in eq.(2.2), the shift does not generate the division by $2\Delta x$. This means, the difference $\Delta z(x, y)$, which is the approximated first derivative of $f(x, y)$, is weighted with the relative shift $2\Delta x$:

$$\Delta z(x, y) = f(x + \Delta x, y) - f(x - \Delta x, y) \approx 2\Delta x f'(x, y) \quad (2.3)$$

This approach was used independently by Alvarez and Lohmann to describe lateral shift tunable optics. The desired function $f(x, y)$ was in both cases a quadratic function, which is a paraxial approximation of the spherical function of optical lenses. While Alvarez' design allows the tuning by a lateral shift parallel to one of the coordinate axes perpendicular to the optical axis [6], Lohmann's design requires a shift in both lateral axes simultaneously [5]. First the mathematical description for a shift of the Alvarez elements is shown:

$$Z_A = \frac{x^3}{3} + xy^2 \quad (2.4)$$

$$\begin{aligned} \Delta Z_A &= \frac{(x + \Delta_A)^3}{3} + (x + \Delta_A)y^2 - \frac{(x - \Delta_A)^3}{3} - (x - \Delta_A)y^2 \\ &= \frac{x^3 + 3\Delta_A^2 x + 3\Delta_A x^2 + \Delta_A^3}{3} + xy^2 + \Delta_A y^2 - \left(\frac{x^3 + 3\Delta_A^2 x - 3\Delta_A x^2 - \Delta_A^3}{3} + xy^2 - \Delta_A y^2 \right) \quad (2.5) \\ &= 2\Delta_A x^2 + 2\Delta_A y^2 + \frac{2\Delta_A^3}{3} \end{aligned}$$

$$\Delta Z_A = 2\Delta_A (x^2 + y^2) + \frac{2\Delta_A^3}{3} = 2\Delta_A Z_A'(x, y) + \frac{2\Delta_A^3}{3} \quad (2.6)$$

The calculation for the Lohmann approach is similar:

$$Z_L = \frac{x^3}{3} + \frac{y^3}{3} \quad (2.7)$$

$$\begin{aligned}
\Delta Z_L &= \frac{(x + \Delta_L)^3 + (y + \Delta_L)^3 - (x - \Delta_L)^3 - (y - \Delta_L)^3}{3} \\
&= \frac{1}{3}(x^3 + 3x^2\Delta_L + 3x\Delta_L^2 + \Delta_L^3) + (x^3 + 3y^2\Delta_L + 3y\Delta_L^2 + \Delta_L^3) \\
&\quad - \frac{1}{3}(x^3 - 3x^2\Delta_L + 3x\Delta_L^2 - \Delta_L^3) - (x^3 - 3y^2\Delta_L + 3y\Delta_L^2 - \Delta_L^3) \\
&= 2\Delta_L x^2 + 2\Delta_L y^2 + \frac{4\Delta_L^3}{3} \\
\Delta Z_L &= 2\Delta_L x^2 + 2\Delta_L y^2 + \frac{4\Delta_L^3}{3} = 2\Delta_L Z_L'(x, y) + \frac{4\Delta_L^3}{3}
\end{aligned} \tag{2.8}$$

$$\tag{2.9}$$

Both approaches lead to the desired tunable function. But the deviation from this idealized function seems to be higher for the Lohmann approach. Actually the deviations are the same since both descriptions can be converted into each other. This is analyzed in detail in the next section.

3. ALVAREZ OR LOHMANN LENSES, OR BOTH?

Luiz Alvarez developed his “two-element variable-power spherical lens” which is defined by equation (3.10) [6]. The focus variation with these elements is achieved by a symmetric displacement of both elements perpendicular to the optical axis z (in this case along the y direction by Δ_A). Independently Adolf W. Lohmann invented “a new class of varifocal lenses” [5]. They are defined by equation (3.11). These elements are also shifted perpendicular to the optical axis to tune their focal length. But the direction of shift in this case is diagonally to the coordinate system; the elements are moved in x and y simultaneously by the same amount Δ_L .

$$Z_A = A_A x^3 + B_A xy^2 \tag{3.10}$$

$$Z_L = A_L x^3 + A_L y^3 \tag{3.11}$$

The apparently different element definitions (eq.(3.10) and (3.11)) describe the same optical functions which can be shown by a coordinate transformation [1]. An Alvarez element rotated by an angle ϕ is described by the new coordinates x' and y' , which are defined by equations (3.12) and (3.13). Inserting these equations the transformed Alvarez description (eq.(3.14)) and expanding it (eq. (3.15) to (3.18)) gives equation (3.19)). Here the equation is arranged by its polynomial terms.

$$x' = x \cos \phi + y \sin \phi \tag{3.12}$$

$$y' = -x \sin \phi + y \cos \phi \tag{3.13}$$

$$Z_A' = A_A x'^3 + B_A x' y'^2 \tag{3.14}$$

$$Z_A' = A_A (x \cos \phi + y \sin \phi)^3 + B_A (-x \sin \phi + y \cos \phi)^2 (x \cos \phi + y \sin \phi) \tag{3.15}$$

$$Z_A' = (x \cos \phi + y \sin \phi)(A_A(x^2 \cos^2 \phi + 2xy \sin \phi \cos \phi + y^2 \sin^2 \phi) + B_A(x^2 \sin^2 \phi - 2xy \sin \phi \cos \phi + y^2 \cos^2 \phi)) \quad (3.16)$$

$$Z_A' = (x \cos \phi + y \sin \phi)(A_A(x^2 \cos^2 \phi + y^2 \sin^2 \phi) + B_A(x^2 \sin^2 \phi + y^2 \cos^2 \phi) + 2(A_A - B_A)xy \sin \phi \cos \phi) \quad (3.17)$$

$$Z_A' = A_A(x^3 \cos^3 \phi + xy^2 \cos \phi \sin^2 \phi + x^2y \cos^2 \phi \sin \phi + y^3 \sin^3 \phi) + B_A(x^3 \sin^3 \phi \cos \phi + xy^2 \cos^3 \phi + x^2y \sin^3 \phi + y^3 \cos^2 \phi \sin \phi) + 2(A_A - B_A)(x^2y \sin \phi \cos^2 \phi + xy^2 \sin^2 \phi \cos \phi) \quad (3.18)$$

$$Z_A' = x^3(A_A \cos^3 \phi + B_A \sin^2 \phi \cos \phi) + y^3(A_A \sin^3 \phi + B_A \cos^2 \phi \sin \phi) + x^2y(3A_A \sin \phi \cos^2 \phi + B_A(\sin^3 \phi - 2 \sin \phi \cos^2 \phi)) + xy^2(3A_A \cos \phi \sin^2 \phi + B_A(\cos^3 \phi - 2 \sin^2 \phi \cos \phi)) \quad (3.19)$$

With the coefficient ratio initially proposed by Alvarez (eq.(3.20)) the angle ϕ can be calculated in a way that the xy^2 and x^2y terms vanish. As expected this is fulfilled for $\phi = 45^\circ$. With equations (3.20) and (3.21) the element description becomes equation (3.23).

$$A_A = \frac{B_A}{3} \quad (3.20)$$

$$\phi = 45^\circ \rightarrow \sin \phi = \cos \phi = \frac{1}{\sqrt{2}} \quad (3.21)$$

$$Z_A' = \frac{x^3}{2\sqrt{2}}\left(\frac{B_A}{3} + B_A\right) + \frac{y^3}{2\sqrt{2}}\left(\frac{B_A}{3} + B_A\right) + x^2y\left(\frac{B_A}{2\sqrt{2}} + B_A\left(\frac{1}{2\sqrt{2}} - \frac{2}{2\sqrt{2}}\right)\right) + xy^2\left(\frac{B_A}{2\sqrt{2}} + B_A\left(\frac{1}{2\sqrt{2}} - \frac{2}{2\sqrt{2}}\right)\right) \quad (3.22)$$

$$Z_A' = \frac{\sqrt{2}B_A}{3}x^3 + \frac{\sqrt{2}B_A}{3}y^3 = Z_L \quad (3.23)$$

From equation (3.23) the relation between the Alvarez and the Lohmann description is indeed a rotation and a scale factor of $\sqrt{2}$, which can be expected due to the rotation angle of 45° :

$$A_L = \frac{\sqrt{2}}{3}B_A = \sqrt{2}A_A \quad \text{and} \quad \Delta_L = \frac{\Delta_A}{\sqrt{2}} \quad (3.24)$$

Since both, the Alvarez and the Lohmann description, are interchangeable, the Alvarez description will be used in this paper for all further considerations.

4. ABERRATIONS IN ALVEREZ-LOHMANN BASED SYSTEMS

The theory behind Alvarez-Lohmann based optical systems relies on an idealized optical model. The two most important assumption are:

- there is no propagation between the individual elements $\delta z_{\text{air}} = 0$, both elements are positioned in the same plane
- the Alvarez lenses are ideally thin, $\delta z_{\text{lens}} = 0$

For the design and fabrication of such systems this means to keep the element thickness and the distance between them as thin as possible. But clearly both thicknesses cannot be reduced to zero. Hence it is interesting to analyze what happens if a distance between the elements and/or a finite element thickness is assumed.

Therefore the first assumption is neglected and finite distances between the thin Alvarez elements are introduced. A wave optical model is used in the next steps, to illustrate and analyze the aberrations resulting in this case [11]. The simulation setup is shown in Fig. 1. A plane wavefront is superimposed onto the first Alvarez element. Then a “spectrum of plane waves” propagation algorithm [12] is used to calculate the resulting wavefront at the plane of the second Alvarez element. Here the resulting wavefront is superimposed onto the second Alvarez element. To make the aberrations of the wavefront visible, the quadratic function resulting from the corresponding ideal setup is subtracted from the wavefront directly in the plane of the second element.

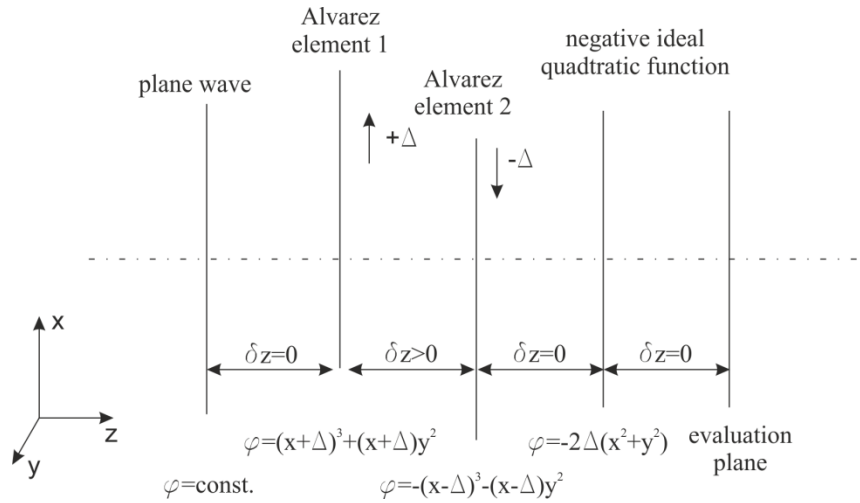


Fig. 1: Simulation setup. Between the first and the second Alvarez element a “spectrum of plane waves” algorithm is used to calculate the propagation of the wavefront. The phase functions of the single elements are written below the corresponding planes.

For the evaluation a pair of Alvarez lenses with a weighting factor of $A_L = 8/\text{mm}^3$ is used. The systems aperture is 10mm and the propagation distance between the Alvarez lenses is $\delta z = 500\mu\text{m}$. As input wavefront a plane wave with a propagation direction parallel to the optical axis is chosen. Fig. 2 shows the resulting wavefront aberrations. A lateral shift of the elements just decenters the aberration as shown in Fig. 2 b). The function itself is not scaled by the lateral shift, unlike the ideal quadratic wavefront. However the aberration function is proportional to the axial distance between the two Alvarez elements [11].

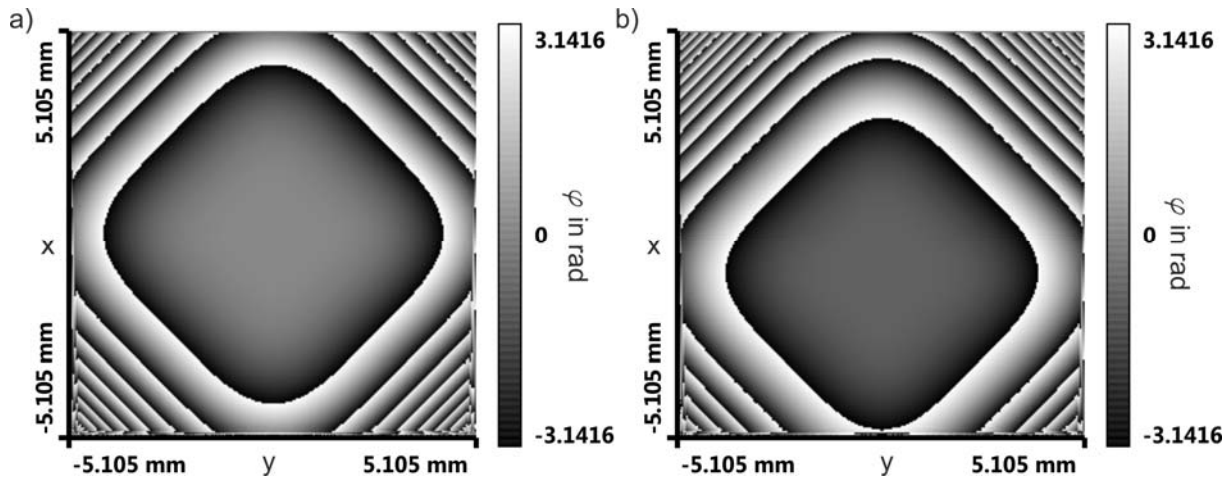


Fig. 2: a) wavefront aberration for zero lateral shift $\Delta = 0$ and b) for a lateral shift of $\Delta=1$ mm

As a plane wave would be the result of this simulation for an ideal system, it becomes clear that the occurring aberrations decrease the image quality of a Alvarez-Lohmann system drastically. Therefore it is necessary to analyze the aberrations and reduce their influence on the system.

5. ANALYZATION AND COMPENSATION OF ABERRATIONS IN ALVAREZ BASED SYSTEMS

To analyze the aberrations in Alvarez Lohmann systems, a polynomial fit is applied to the distorted wavefront. The polynomial coefficients are then weighted inverse to their polynomial order. This way the most influencing terms are found. Since in the example above the aberrations are insensitive to the lateral shift, they are caused solely by the propagation between the Alvarez elements. Hence they have to be compensated for at the first element only. Therefore the inverse aberration function is superimposed onto the function of the first element and weighted by an optimization factor [11]. The results of such an optimization are shown in Fig. 3.

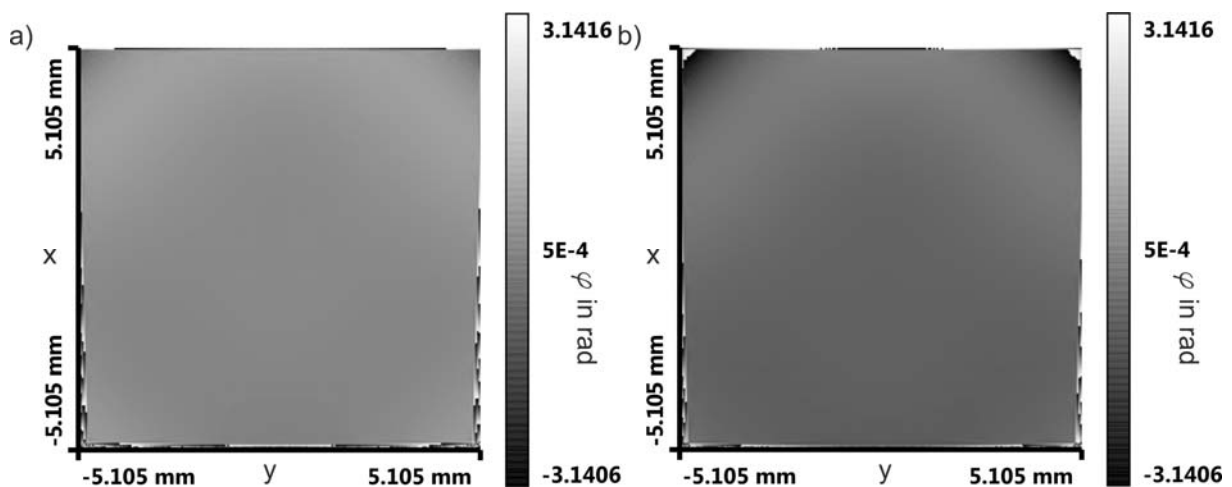


Fig. 3: a) wavefront aberration of the optimized model for zero lateral shift $\Delta = 0$ and b) for a lateral shift of $\Delta=1$ mm

However this optimization yields best results only for one single field angle. In Fig. 4a the wavefront deviation for a field angle of 5° is shown. An on-axis optimization as used in Fig. 3 in this case reduces the aberration also for the field but not as efficiently as for the axis (Fig. 4b). This is a common problem in lens design. An optimization process is used to find an equilibrium between all field angles. To increase the degree of freedom for the optimization more complex polynomial descriptions for the Alvarez elements are used.

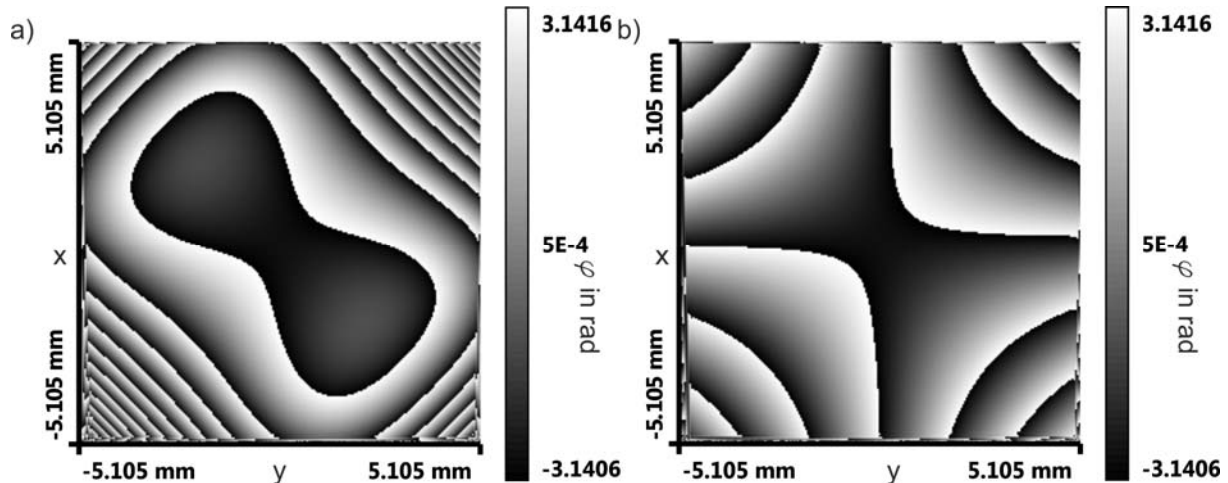


Fig. 4: a) wavefront aberration for the initial model at 5° field and for zero lateral shift $\Delta = 0$ and b) for the on axis optimized model

As a next step towards a more realistic system model finite element thicknesses are introduced. This also introduces multiple aberrations. Especially aberrations, which scale with the lateral shift of the elements makes it necessary to adjust the polynomial descriptions of both Alvarez elements [13].

To tackle this challenges ray tracing simulations are used to model the systems. The results from the wavefront analysis are incorporated for the design of a starting system. An extended merit function is used to ensure the functionality and moreover the fabricability of the elements. A system optimized this way is presented in the next section.

6. CONFOCAL HYPERSPECTRAL IMAGING SYSTEM WITH OPTIMIZED ALVAREZ LENSES

6.1 Concept and Design

Confocal hyperspectral imaging incorporates the longitudinal chromatic aberration of an optical system to separate the spectral components of light. [14-16].

The dispersion characteristics of optical media (e.g. glass or plastics) describe the wavelength dependency of the index of refraction $n(\lambda)$. As a result of this dependency, a lens focuses light of different wavelength at different positions along the optical axis. A pinhole positioned in a wavelength corresponding focal plane will efficiently attenuate all wavelengths which are out of focus at this plane. Hence a sensor behind the pinhole will only detect light from a specific wavelength. This concept can be enhanced to multiple field points by the use of a pinhole array. [17, 18]

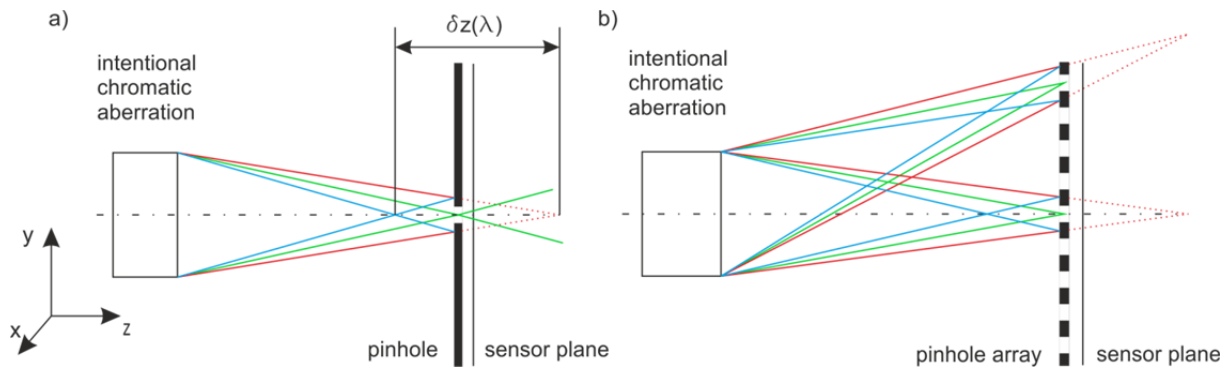


Fig. 5: a) Chromatic confocal concept: the systems focal length is a function of the wavelength; only the wavelength which is ideally focused in the pinhole plane passes the pinhole unattenuated. b) The principle can be extended to full field by the implantation of pinhole arrays

The whole spectrum of the incoming light can be analyzed by changing the focal length of the lens, such that sequentially all wavelengths are in focus at the pinhole plane. Alvarez Lohmann lenses are, due to their compact design, ideal for the focus tuning. The target hyperspectral system consists of a collimating optic, which images a first pinhole array at a infinite distance. An Alvarez-Lohmann element pair is used to separate the spectral bands and tune the focus length, and hence the wavelength in focus.

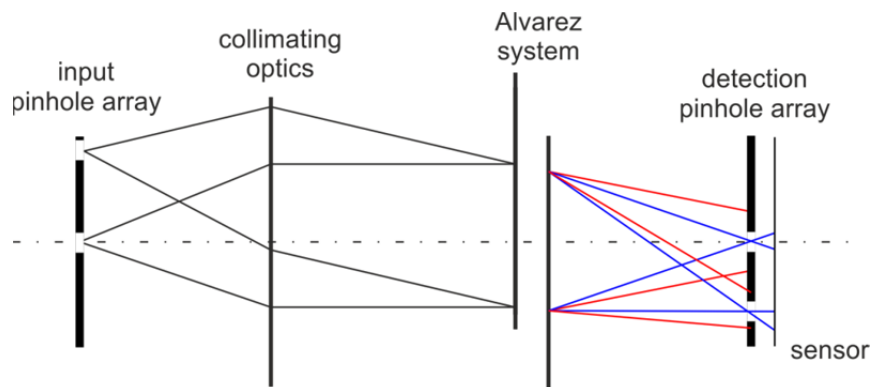


Fig. 6: Schematic of the optical layout of the hyperspectral system based on Alvarez Lohmann lenses. The wavelength, which is in focus at the detection pinhole array, is tuned by a lateral shift of the Alvarez-Lohmann lenses.

For the systems model, the collimating optics is assumed to be ideal. The Alvarez Lohmann lens is optimized for a plane incident wave. The design parameters for the Alvarez system are summarized in Tab. 1 [19].

	Lens Data	
	desired	achieved
Spectral range	450– 750 nm	450 – 750 nm
Numerical aperture	> 0.05	0.052 – 0.054
Maximum field angle	$\geq 3^\circ$	3°
Spot radius	< 10 μm	4.4 μm rms
Long. Chromatic aberration	2 mm	1.85 mm

Tab. 1: Design goals and achieved parameters for the hyperspectral system

To achieve a large longitudinal chromatic aberration the thickness of the Alvarez elements needs to be high. As explained above, this leads to increased aberrations. For the design an asymmetric starting system was chosen. Polynomial coefficients up to the 7th order were optimized on both elements to minimize the aberrations and reach the design goals shown in Tab.1. The desired rms spot size below 20 μm results from the diameter of the pinholes. Another important design criterion is a constant magnification of the system for all tuning states. Both goals are reached by the design as can be seen in Fig. 7, where the spot diagrams for different field angles and tuning states are presented. The image point positions stay constant over the whole tuning range.

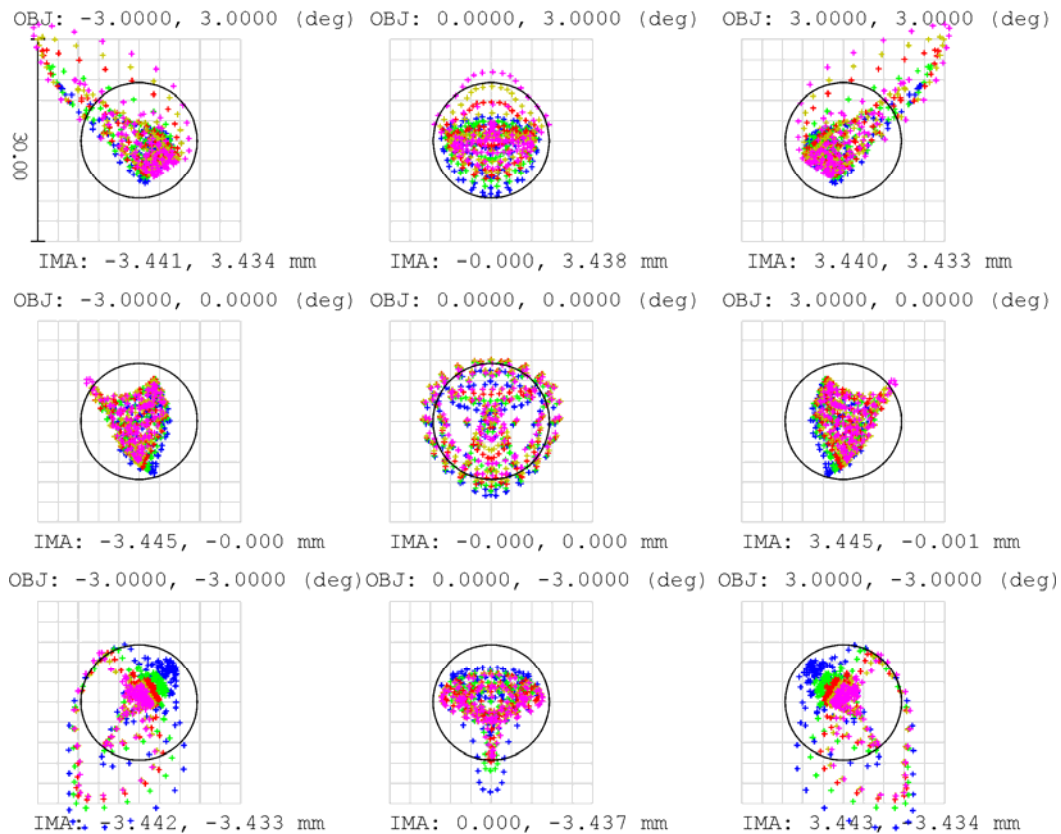


Fig. 7: Spot diagrams of the hyperspectral Alvarez system for different field points; the circle indicates the Airy radius of 8.5 μm

6.2 Fabrication

PMMA was chosen as material for the Alvarez lenses. This material has excellent characteristics as substrate for diamond machining technologies. Since the designed Alvarez lenses are non-rotational symmetric freeform elements a precision micro milling process was used for their fabrication. Direct tool path programming uses the analytical polynomial description of the elements to calculate the tool trajectory on the fly while the process is running. This way the data volume for the milling machine is reduced significantly. Also fabrication parameters can be adjusted any time while the process is running to increase the quality of the resulting elements. In Fig. 8 the optical functionality of the fabricated elements is demonstrated on a parallel bar grid. To enlarge the chromatic aberration, the Alvarez Lohmann lenses can be fabricated as diffractive optical elements (DOEs). A major advantage of the DOE approach is a significant reduction of the element thickness and the distance between the elements. This results in a decrease of aberrations and therefore in an improvement of the overall system performance [13, 17, 20].

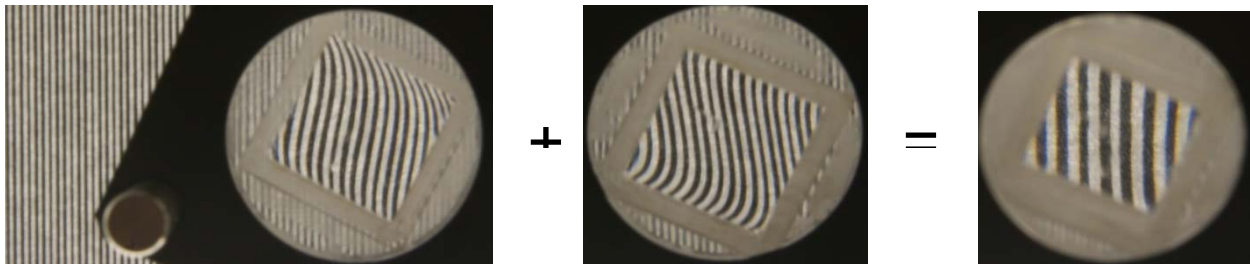


Fig. 8: left) bar grid imaged through the first Alvarez element. The distortion of the bars results from the desired surface function of the elements, middle) bar grid imaged through second element; right) bar grid imaged through the combined elements – the desired quadratic phase is demonstrated by the undisturbed, magnified bars

7. CONCLUSION

In this paper the idealized concept of Alvarez Lohmann lenses was explained. Furthermore it was shown, that the approach of Alvarez and the approach of Lohmann can be converted into each other by a coordinate transformation. Aberrations which are introduced by violations of the idealized model are analyzed by a wave optics approach. To optimize Alvarez Lohmann lenses for multiple field points and thick elements, ray tracing simulations were incorporated. As an example for such an optimization, a hyperspectral imaging system using tunable optical elements on basis of Alvarez-Lohmann lenses was presented.

REFERENCES

- [1] S. Barbero, “The Alvarez and Lohmann refractive lenses revisited.” *Optics express* **17**, 9376–90 (2009).
- [2] S. Barbero and J. Rubinstein, “Power-adjustable sphero-cylindrical refractor comprising two lenses,” *Optical Engineering* **52**, 063002 (2013).
- [3] S. Bernet, W. Harm, and M. Ritsch-marte, “Demonstration of focus-tunable diffractive Moiré-lenses,” *Optics express* **21**, 4317–4322 (2013).
- [4] E. Acosta and J. Sasián, “Phase plates for generation of variable amounts of primary spherical aberration.” *Optics express* **19**, 13171–8 (2011).
- [5] A. Lohmann, “A new class of varifocal lenses.” *Applied optics* **9**, 1669–71 (1970).
- [6] L. W. Alvarez; “Two-Element variable-power spherical lens” US Patent 3,305,294 (1967).
- [7] S. Stoebenau, R. Kleindienst, M. Hofmann, and S. Sinzinger, “Computer-aided manufacturing for freeform optical elements by ultraprecision micromilling,” in “SPIE Optical manufacturing and testing IX,” (2011), p. 12.
- [8] S. Sinzinger, “Optical freeform surfaces in integrated optical microsystems (Invited Talk),” in “Imaging and Applied Optics Technical Papers,” (OSA Technical Digest (online), Monterrey, CA, 2012).
- [9] A. Lohmann and S. Sinzinger, “Moiré effect as a tool for image processing,” *J. Opt. Soc. Am. A* **10**, 65–68 (1993).
- [10] A. Lohmann and D. Paris; “Variable Fresnel Zone Pattern”; *Applied optics* **6**, 1567-1570 (1967).

- [11] A. Grewe, M. Hillenbrand and S. Sinzinger; "Aberrations in tunable optical systems based on Alvarez-Lohmann lenses" **submitted to Applied optics**
- [12] J. Goodman, *Introduction to Fourier Optics* (McGraw-Hill, 1996), 2nd ed.
- [13] A. Grewe, M. Hillenbrand, C. Endrödy, M. Hoffmann, and S. Sinzinger, "Advanced phase plates for confocal hyperspectral imaging systems," in *Imaging and Applied Optics*, OSA Technical Digest (online) (Optical Society of America, 2013), paper AW1B.2.
- [14] K. Körner; „Verfahren und Anordnung zur schnellen, orts aufgelösten, flächigen, spektroskopischen Analyse, bzw. zum Spectral Imaging oder zur 3D-Erfassung mittels Spektroskopie“; Patent DE102006007172 B4 , 2006
- [15] M. Hillenbrand, A. Grewe, M. Bichra, B. Mitschunas, R. Kirner, R. Weiß, and S. Sinzinger; "Chromatic information coding in optical systems for hyperspectral imaging and chromatic confocal sensing"; In: Proc SPIE 8550, 85500D (2012).
- [16] M. Hillenbrand, A. Grewe, M. Bichra, R. Kleindienst, L. Lorenz, R. Kirner, R. Weiß, and S. Sinzinger; "Parallelized chromatic confocal sensor systems"; In: Proc SPIE 8788, 87880V (2013).
- [17] A. Grewe, M. Hillenbrand and S. Sinzinger; "Adaptive confocal approach to hyperspectral imaging." - In: EOS annual meeting 2012 (EOSAM 2012) / EOS (European Optical Society) annual meeting; (Aberdeen): 2012.09.25-28. - Hannover: EOS, European Optical Society (2012),
- [18] A. Grewe, M. Hillenbrand and S. Sinzinger; "Optimized Alvarez phase plates for hyperspectral imaging." - In: DGaO-Proceedings. - Erlangen-Nürnberg: Dt. Gesellschaft für angewandte Optik: ISSN 16148436 (2012),
- [19] A. Grewe, M. Hillenbrand and S. Sinzinger; "Hyperspectral imaging sensor systems using tunable lenses". - In: Photonik international ...; trade journal on optical technologies; selected photonik articles republished in English; best of. - Stuttgart: AT-Fachverlag, ISSN 14329778, Bd. 8 (2013), S. 2-5
- [20] A. Grewe, C. Endrödy, R. Fütterer, P.H. Cu-Nguyen, S. Steiner, M. Hillenbrand, M. Correns, M. Hoffmann, G. Linß, H. Zappe and S. Sinzinger; "Opto-mechanical microsystems for hyperspectral imaging sensors." - In: Microsystems technology in Germany. - Berlin: Trias Consult, ISSN 21917183 (2014)

CONTACTS

Dipl...-Ing. Adrian Grewe
 Prof. Dr. rer. nat. habil. Stefan Sinzinger

adrian.grewe@tu-ilmenau.de
stefan.sinzinger@tu-ilmenau.de